Reply on co-editor's comments

1. Moisture Budget and Mass Balance

Following the points raised by Reviewers 2 and 6, I would like to look closer at the moisture sourcing. In the discussion of the moisture sources for these ARs, it is suggested that the sea surface (for the Atlantic AR) and soil moisture (for the Eurasian AR) act as the primary sources. However, in the provided uptake/loss difference maps (Figs. 9c and 12c), there appears to be a spatial imbalance where moisture loss significantly exceeds local uptake along the trajectories for both events. I suggest calculating the spatial mean of the difference plots to see if the budget closes near zero.

As discussed in the revised version, it can be suggested that a substantial portion of the moisture may have already been in the atmosphere before the start of the back-trajectories - can they be extended? Furthermore, as Reviewer 6 questioned, if the parcels have not been in contact with the surface during the tracked window, the mechanism for moisture acquisition remains unclear - please discuss these mechanisms in the text.

Thank you for this comment. As you correctly note, moisture loss exceeds moisture uptake along the trajectories. This reflects the properties of the air parcels at the time of being incorporated into the AR. The parcels originate in the mid-latitudes and therefore have humidity values typical of those regions. As they travel poleward, the parcels source additional moisture from the surface and experience substantial moisture loss when reaching their endpoints. Importantly, Lagrangian air parcel trajectory analysis is designed to diagnose the evolution of parcel properties and identify relative source and sink regions, rather than to provide a closed moisture budget for the AR as a whole. For this reason, exact closure between moisture gain and loss along trajectories is not expected, especially as parcel humidity reflects pre-existing atmospheric moisture and may be influenced by mixing and spatio-temporal sampling choices. We acknowledge that the term 'budget' had been used in the manuscript on several instances which has now been revised accordingly.

Nonetheless, to address your question specifically, parcels reaching the Greenland coast have an average specific humidity of 2.96 g/kg five days prior to their endpoints (see manuscript Fig. 8). Along their pathways, they gain moisture from the underlying surface, reaching an average maximum moisture content of 4.17 g/kg 2-3 days before arrival, before decreasing to 0.84g/kg at the endpoint. Over the full five-day period, each parcel thus loses on average 2.12g/kg of moisture, indicating that moisture loss outweighs the moisture gain. Parcels reaching the central Arctic undergo a similar evolution with moisture content increasing from 1.97 g/kg seven days before arrival to 2.38g/kg and then decreases to 0.54g/kg at the endpoint (see Fig. 11).

As mentioned in the Methods section, we performed LAGRANTO back trajectory calculations for 9 days and selected region-specific trajectory lengths based on AR lifetime and the evolution of key parcel properties. For your information and completeness, we also examined the full nine-day trajectories. For the nTpθ group identified as AR-related parcels, temperature, potential temperature, specific humidity, pressure and latitude all remain nearly constant during the first four days for parcels reaching the Greenland coast, and the first two days for those reaching the central Arctic. From day –5 and –7, respectively, the parcels start to show increases in specific humidity and temperature. This indicates that the pre-AR period is well-captured and that extending the trajectories further does not recover additional or changes in moisture sources. The initial moisture

content therefore reflects pre-existing atmospheric humidity rather than surface uptake outside the selected trajectory time window.

Our understanding is that reviewer 6 refers to the pTpθ and pTnθ subgroups reaching the Greenland coast. These parcels are typically located at pressures < 650hPa and therefore do not interact with the surface. However, the nTpθ subgroups reaching both the Greenland coast and the central Arctic travel in the lower levels of the atmosphere. In regions of moisture uptake, the parcels descend to around 900 hPa, allowing direct interaction with the PBL and surface.

We have added a sentence to the manuscript explaining why moisture loss exceeds moisture uptake: '*Note that moisture loss exceeds moisture uptake as the initial moisture content of the parcels reflects the pre-existing atmospheric moisture of their mid-latitude origin region, which is subsequently lost during poleward transport in addition to the moisture gained through surface fluxes along the trajectory.'* See lines 377-380 on page 17.

Property evolution for parcels reaching the Greenland coast

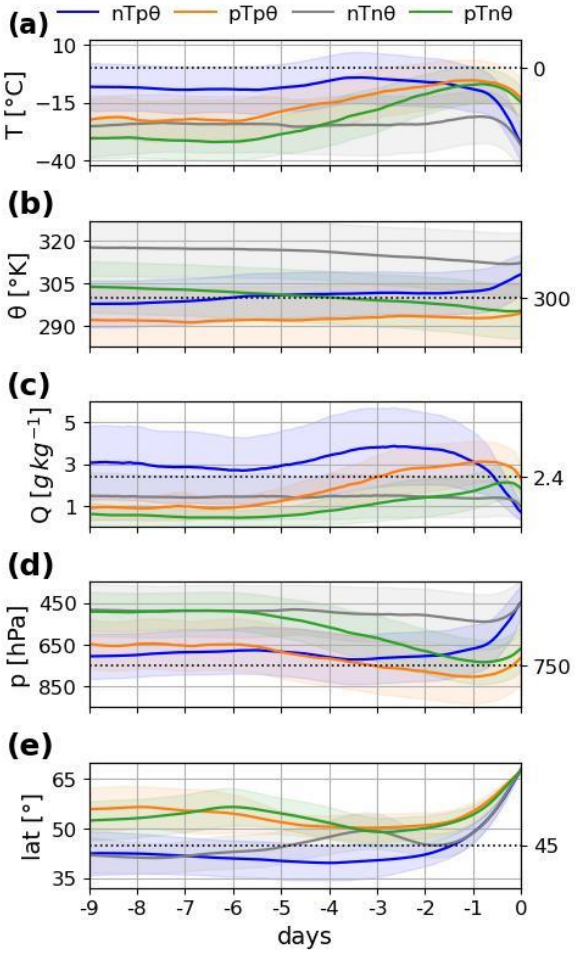

Property evolution for parcels reaching the central Arctic

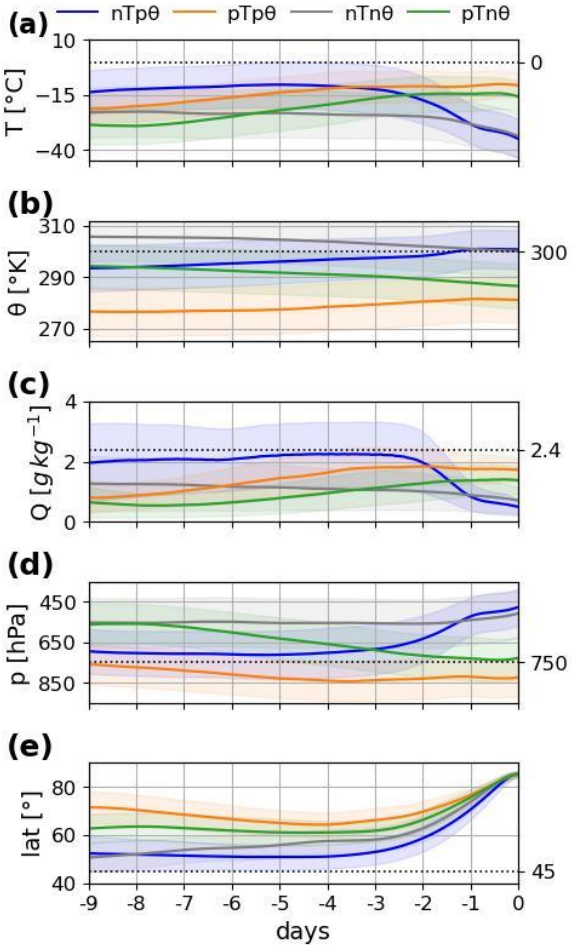

2. Synoptic Drivers vs. Upper-Level Dynamics
The current synoptic discussion relies heavily on MSLP couplets to describe the conditions. However, wave trains are typically an upper-level phenomenon. It would be beneficial to the physical narrative to examine the upper-level flow. Was there a Rossby Wave Breaking along the trajectories?

Thank you for this comment. We have carried out the requested analyses and decided to submit these additional results as *Appendix A* as they appear to enhance the mechanistic understanding of the synoptic drivers. We have also added the following to the manuscript: 'Further analysis suggests that the extreme regional MSLP anomalies shown in Fig. 2 involve an upper-level wave train near the tropopause that is likely coupled with surface cyclogenesis. See Appendix for additional information.' See lines 230-331 on page 10.

Appendix A: Influence of upper-level flow on AR dynamics

To assess the role of upper-level dynamics, we examine the Ertel potential vorticity (PV) at 12 UTC on the 315 K isentropic surface during 13-21 April 2020 (Fig. A1). The 315 K surface is representative of the mid latitude tropopause, where Rossby wave activity and wave breaking are typically strongest. High PV values indicate air of stratospheric origin while low PV values indicate tropospheric or lower latitude air.

It is evident from Fig. A1 that a synoptic-scale upper-level wave train is present over the North Atlantic and Eurasian sectors. Both cyclonic and anticyclonic wave breaking are evident, with filaments of high- and low-PV air becoming partially detached and mixed. However, the AR pathways are not consistently collocated with the detached filaments or with the clearest PV overturning features. Instead, the ARs tend to follow the sharp PV gradient along the western edge of the low-PV region, before recirculating around the low-PV region over the central Arctic. This suggests that the ARs may have been steered by the upper-level wave train along the regions with sharp negative PV gradient, while wave breaking mainly contributes to deepening and maintaining the quasi-stationary wave train. Fig. A1 therefore does not support a one-to-one correspondence between individual wave-breaking tongues and poleward AR intrusions.

To further assess the extremity of the upper-level flow, we analyse the mean PV anomaly for the target period 15-21 April 2020 relative to the 1979-2023 climatology (Fig. A2). A quasi-stationary wave train poleward of 40°N is evident. We define regional boxes enclosing each positive and negative PV anomaly centre associated with the ARs. For the Atlantic AR, the positive PV anomalies over North America (red box) is highly unusual, lying at the 95.9th percentile of the climatological distribution. The anomalously low PV over the North Atlantic (blue box) corresponds to the 1.2nd percentile of the distribution. In contrast, the Eurasian AR is associated with a region of anomalously high PV over western Europe (pink box) that corresponds to the 70.4th percentile, whereas the negative PV anomaly over northern Siberia (cyan box) is exceptionally rare, being the 0.4th

percentile of the distribution. This indicates that the Eurasian AR event is distinguished primarily by an extreme intrusion of low-PV air into the high Arctic on the 315 K surface, consistent with strong poleward transport of anticyclonic upper-tropospheric air.

In addition, the extreme positive PV anomalies over North America are well placed to reinforce the further south-east located quasi-stationary driving cyclone (see Fig. 1). Through PV inversion, such an upper-level anomaly supports cyclonic circulation, favours ascent downstream, and helps maintain low MSLP (Hoskins et al., 1985). The downstream block over the North Atlantic likely strengthens this coupling by slowing eastward Rossby wave propagation and maintaining the persistent trough-ridge configuration shown in Fig. A2. Together, the upstream positive PV anomaly and the downstream negative PV anomalies likely contributed to the persistence of the driving cyclone, although any deepening would still depend on low-level baroclinicity and diabatic processes (Davis and Emanuel, 1991). These results suggest that the Arctic AR intrusions are more likely driven by a coupled interaction between surface cyclogenesis and the upper-level wave train, rather than by surface processes or upper-level dynamics alone.

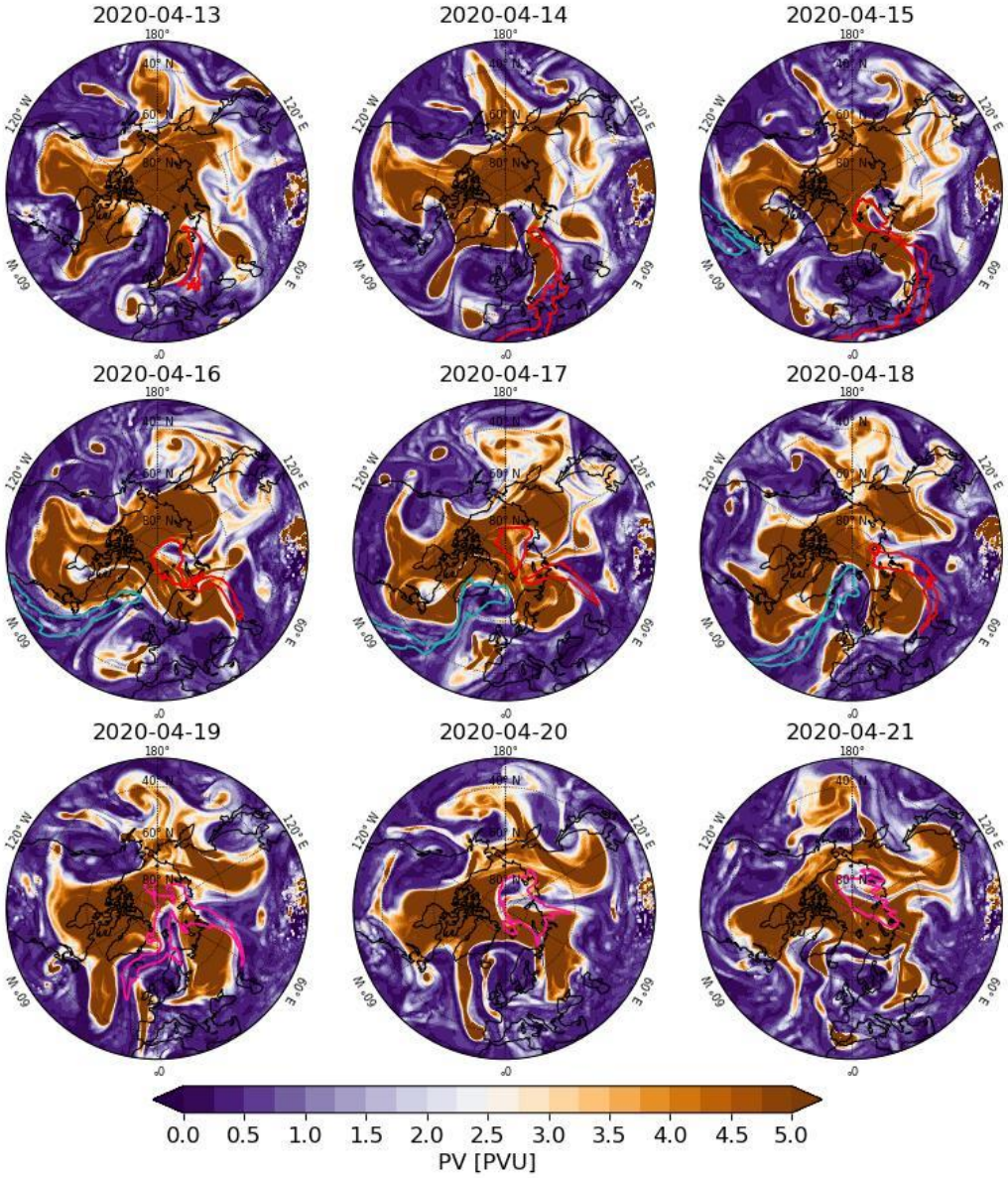

Figure S1: Ertel PV on the 315 K isentropic surface at 12:00 UTC for 13–21 April 2020 (shading) based on ERA5 data. Red and teal contours delineate the boundaries of the Eurasian and Atlantic ARs, respectively, as diagnosed from the tARget database at 12:00 UTC each day. Following the merger of the two ARs, their combined boundary is shown in pink.

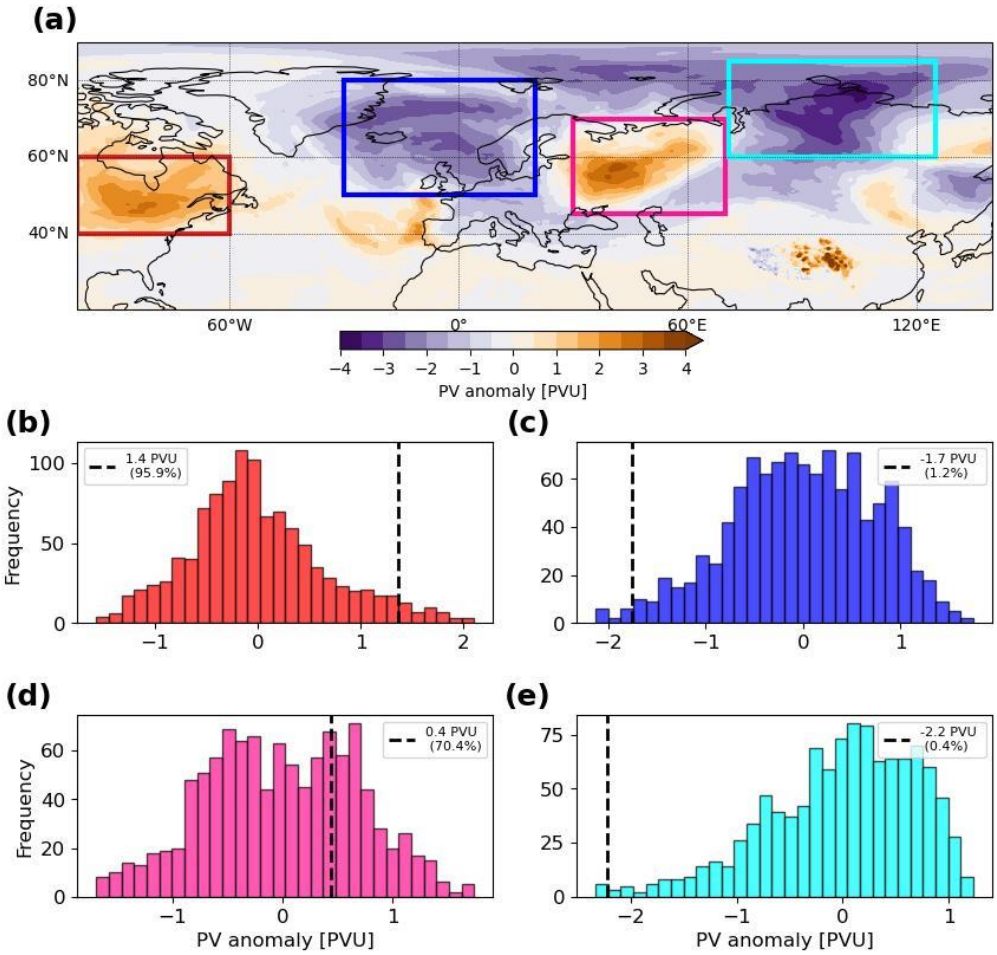

Figure S2: (a) 7-day mean PV anomalies averaged over 15–21 April 2020 relative to the April climatology based on ERA5 data. Boxes denote the centres of action of the quasi-stationary wave train, defined over the following regions: 60°–100°W, 40°–60°N (red); 30°W–20°E, 50°–80°N (blue); 30°–70°E, 45°–70°N (pink); and 70°–125°E, 60°–85°N (cyan). (b) Distribution of 7-day mean PV anomalies for April 1979–2024, averaged over the region enclosed by the red box in (a). The value for the target period is indicated by a black dashed line with its percentile and magnitude shown in the legend. (c–e) As in (b), but for the blue, pink, and cyan boxes in (a), respectively.

3. Minor edit

... and intense precipitation along the Greenland coast and in the central Arctic. The events coincided with a notable decline in sea ice extent in the Barents-Kara Sea and along eastern Greenland...(abstract)

Please keep the same order of geographical regions.

Thank you for pointing this out. The text now reads: '*The events coincided with a notable decline in sea ice extent along eastern Greenland and in the Barents-Kara Sea, that is highly correlated with the AR-induced warming and rainfall.*' See lines 10-11 on page 1.

4. Acknowledgments

Finally, I softly suggest acknowledging the observational efforts of the Polarstern and its crew - a brief acknowledgment of the mission would be appropriate.

We agree that an acknowledgement of MOSAiC and its crew should be included. We have added the following to the acknowledgement section: *'Finally, we thank all those who contributed to MOSAiC and made this endeavour possible (Nixdorf et al., 2021).'*